11th Australasian Fluid Mechanics Conference
University of Tasmania, Hobart, Australia
14-18 December 1992

A NUMERICAL INVESTIGATION OF THE NONLINEAR INTERACTION OF SHORT INTERNAL WAVES WITH INERTIAL WAVES

C. MACASKILL[1] and D. BROUTMAN[2]

[1]School of Mathematics & Statistics, University of Sydney, NSW 2006, AUSTRALIA

[2]School of Mathematics, University of New South Wales, Kensington, NSW 2033, AUSTRALIA

ABSTRACT

Throughout the world's oceans there is internal wave activity. Extensive measurements have shown that velocity and temperature spectra are well-described by a universal form, (see, e.g. Garrett and Munk, 1979). The Garrett-Munk model is essentially empirical, and does not take into account many processes which are believed to control spectral shape and energy levels, such as nonlinear interactions and refraction by currents.

A Fourier spectral model has been developed to investigate some new processes that are likely to have an important influence on the high wavenumber part of the internal wave spectrum. These short waves are probably responsible for most of the dissipation of internal-wave energy, and are strongly refracted by the large-amplitude inertial waves that are present at all depths in the ocean. The interaction between short waves and inertial waves is studied numerically and agreement is found with the predictions from ray calculations. It is then demonstrated that the refraction process generates a vertical wavenumber spectrum consistent with an m^{-2} power law (where m is vertical wavenumber), in a time corresponding to only a few inertial periods.

1. INTRODUCTION

In this paper the interaction of an inertial frequency, large amplitude wave with a short internal wave packet is treated using a spectral approach. Periodic boundary conditions are imposed, and Fourier transform techniques are used to approximate spatial derivatives. A high order Runge-Kutta time integration scheme is used, which ensures a large stability limit. In particular the effects of rotation are discussed and contrasted with the non-rotating case (Winters and D'Asaro, 1989). To include such rotation, we require a three-dimensional velocity field. However, the model is reduced to a simpler form where only two-dimensional interactions need be treated by retaining all three velocity components, but making all flow variables independent of the third dimension, an idea used in a similar context by Holloway (1984).

There are a number of assumptions made in this model. As stated above, all interactions are two dimensional only, so that all energy is contained in modes that lie in a vertical plane. The inertial flow has no horizontal dependence at all; though idealized, this is consistent with the internal-wave dispersion relation for waves of inertial frequency. In addition, the amplitude of the background inertial wave is significant but not large by oceanographic standards, and the internal wave packet has relatively small amplitude. Despite this, amplitudes are large enough to display some of the more interesting refractive changes described in the ray theories of Broutman (1984, 1986) and Broutman and Young (1986) but small enough to ensure that no wave-breaking takes place. It is shown that the basic mechanisms described in these papers are the appropriate ones for the simple flows described here. On the other hand, features not previously described in such flows, particularly the evolution of the time frequency and wavenumber energy spectra, show interesting similarities with the more complicated internal wave evolution models, such as those of Henyey et al (1986) and Shen and Holloway (1986) (see also the review by Müller et al, 1986). In particular, it is found that the vertical wavenumber spectra evolve very quickly, as opposed to the horizontal wavenumber spectra, which are essentially unchanging in time, so long as there is initially no horizontal dependence in the near inertial background velocity field and the internal wave amplitudes are moderate. In addition the high wavenumber, vertical wavenumber spectra evolve over several inertial periods to a power law form, independent of the detailed dynamics. By contrast the low wavenumber part of the vertical wavenumber spectrum is more sensitive to the precise form of the initial short internal wave packet, in particular its dominant vertical wavenumber.

Thus the high wavenumber structure is shown to be due to the refraction of short waves by the large scale background (inertial) flow and hence may be predicted by first order ray theory. In particular, the observed density perturbations may be predicted in this way. By contrast, small-scale nonlinear interactions generate perturbation velocities at the inertial frequency by mechanisms similar to those of wave-mean flow interaction, as described by Broutman and Grimshaw (1988). These perturbations are found in the horizontally averaged motions.

2. FORMULATION

On taking cartesian coordinates (x, y, z) with z vertically upwards, making the Boussinesq approximation, and ignoring derivatives in the $y-$ direction, the equations of motion are

$$\begin{aligned}
&\frac{\partial u}{\partial t}+u\frac{\partial u}{\partial x}+w\frac{\partial u}{\partial z}-fv-\nu\nabla^2 u=-\frac{\partial \phi}{\partial x}\\
&\frac{\partial v}{\partial t}+u\frac{\partial v}{\partial x}+w\frac{\partial v}{\partial z}+fu-\nu\nabla^2 v=0\\
&\frac{\partial w}{\partial t}+u\frac{\partial w}{\partial x}+w\frac{\partial w}{\partial z}+\sigma-\nu\nabla^2 w=-\frac{\partial \phi}{\partial z}.
\end{aligned} \tag{1}$$

Here $\phi = p/\rho_0$. The fluid velocity is $\mathbf{u} = (u, v, w)$, p is pressure and ρ is density, where $\rho = \rho' + \rho_0$ with $\rho_0(z)$ the mean density profile. Since the buoyancy frequency N is assumed constant, and $N^2 = -\frac{g}{\rho_0}\frac{d\rho_0}{dz}$ the mean density increases exponentially with depth. Here g is the acceleration due to gravity, which acts downwards, and ν is the kinematic viscosity. In the ∇^2 operator, $y-$derivatives have also been set to zero.

The inertial frequency is f. Note that in the absence of rotation, where $f = 0$, there are no contributions from the velocity v and it may be ignored. Finally $\sigma = \frac{g\rho'}{\rho_0}$, the scaled density perturbation due to the presence of internal wave motions, satisfies

$$\frac{\partial \sigma}{\partial t}+u\frac{\partial \sigma}{\partial x}+w\frac{\partial \sigma}{\partial z}-N^2 w+Pr^{-1}\nu\nabla^2\sigma=0, \tag{2}$$

which has been derived with use of the continuity condition $\nabla \cdot \mathbf{u} = 0$. The Prandtl number Pr is defined by $Pr = \frac{\nu}{\kappa}$, where κ is the thermal diffusivity, and is assumed to be equal to one henceforth.

A vorticity-stream function formulation is employed, where the stream function ψ is defined by

$$u = \psi_z \qquad \text{and} \qquad w = -\psi_x.$$

The three-dimensional definition of vorticity is employed, where the vorticity vector is given by the curl of the velocity vector. The equations (1) and (2) then become

$$\begin{aligned}
&\frac{\partial \zeta}{\partial t}-J(\psi,\zeta)-\frac{\partial \sigma}{\partial x}-f\frac{\partial v}{\partial z}-\nu\nabla^2\zeta=0\\
&\frac{\partial v}{\partial t}-J(\psi,v)+fu-\nu\nabla^2 v=0\\
&\frac{\partial \sigma}{\partial t}-J(\psi,\sigma)-N^2 w-\nu\nabla^2\sigma=0,
\end{aligned} \tag{3}$$

where the Jacobian $J(a,b) = \frac{\partial a}{\partial x}\frac{\partial b}{\partial z} - \frac{\partial b}{\partial x}\frac{\partial a}{\partial z}$, and where $\zeta = u_z - w_x$ is the $y-$ component of vorticity.

The solution procedure involves time-stepping equation (3), using old values of $(u, v, w), \psi, \zeta$ and σ at timestep n, say, to determine ζ, v and σ at timestep $n+1$. Then the Poisson equation $\zeta = \nabla^2\psi$ is solved, using Fourier methods, to find the stream function at time $n+1$, and hence u and w, the velocity components in the vertical plane, may be determined by differentiation, again using a spectral approach.

A splitting technique is used for the dissipative terms. Thus for each Runge-Kutta time-step, the equations are first solved ignoring dissipation. Consider, for example, the vorticity equation. At the end of each step, the equation

$$\frac{\partial \zeta}{\partial t} - \nu\nabla^2\zeta = 0, \tag{4}$$

is solved exactly over (t_n, t_{n+1}) by taking the Fourier transform to find

$$\frac{\partial \tilde{\zeta}}{\partial t} + 4\pi^2(k^2+m^2)\nu\tilde{\zeta} = 0, \tag{5}$$

where $\tilde{\zeta}$ is the Fourier transform of ζ, and k and m are the horizontal and vertical wavenumbers respectively. Equation (5) is then solved directly and an inverse transform taken to find ζ. A similar approach is used for v and σ. Thus the dissipation enters as a Gaussian filter at each time step.

The equations are solved in a box, depth $l = 100$m and width w $= 100$m. Periodic boundary conditions are imposed in both the $x-$ and $z-$ directions. The background inertial wave is chosen to have the form

$$\begin{aligned}
(u, v) = U_0 &\exp(-a_1^2(z/l - 1/2)^2)\\
&\times(\cos(\beta z - ft), \sin(\beta z - ft)),
\end{aligned} \tag{6}$$

where the envelope constant $a_1 = .1$ for these simulations, and $\beta = 2\pi/l$, so that the wavelength of the inertial wave is equal to the depth of the domain. The velocity scale $U_0 = .03$ m/sec. The inertial wave thus gives rise to a time-varying shear, localized near the middle of the computational box. There is initially no horizontal variation in the background flow. The initial short internal wave packet is set up in a similar fashion, with the horizontal wavelength equal to the width of the box, and the vertical wavelength one sixth of this, i.e. $m/k = -6$ (the minus sign gives group propagation upwards). The vertical velocity of the internal wave packet is given by

$$w = AG(z)\sin(kx + mz - \omega t), \tag{7}$$

where the envelope function $G(z)$ for the internal wave packet is of the form

$$G(z) = \exp(-a_2^2(z/l - 1/4)^2) \tag{8}$$

with $a_2 = .075$. For the simulations discussed here the maximum vertical velocity of the internal wave packet is 2.8×10^{-3} m/sec. The initial horizontal velocities u and v and the perturbation density σ have a similar form to (7) and are determined by finding the plane wave solution to the equations (1) and (2) with the advection and dissipative terms set to zero, and then applying the envelope $G(z)$ as in (8).

The intrinsic frequency ω of the internal wave packet is given by the internal wave dispersion relation

$$\omega^2(k,m) = \frac{N^2k^2 + f^2m^2}{k^2+m^2}. \tag{9}$$

For the results given below the inertial frequency $f = .0001$ radians/sec, and the buoyancy frequency $N = .005$ radians/sec. The calculations were performed on a grid of size 48×1024, with 4000 timesteps per day. A realistic oceanic value of the viscosity $\nu = 10^{-6}$m^2/sec was used. For internal wave packets with greater amplitudes, a much larger value of (artificial) viscosity would be required to suppress numerical instabilities, and in fact Winters and D'Asaro (1989) resorted to the use

of 'hyperviscosity' to resolve their very large amplitude cases.

3. RESULTS

In Figure 1, we present the perturbation density as a function of depth and time, at the fixed horizontal location of one quarter of the box width. The inertial wave packet does not appear directly in this figure, as there is no corresponding density perturbation, but rather only a horizontal velocity perturbation. The small-scale internal wave packet can be seen propagating upwards and then interacting with the inertial flow in the centre of the box after about a quarter of a day. Very strong refraction takes place, but after about three quarters of a day the short internal wave packet escapes. Because of the periodic boundary conditions, further interactions with the inertial wave take place over the next day or so. By contrast, with this fairly low value of the internal wave amplitude, one sees almost total absorption at the critical layer if the time varying shear is replaced with a uniform shear of similar magnitude, as in Winters and D'Asaro (1989). (The critical level in the non-rotating case is the depth at which the internal wave horizontal phase velocity is equal to the horizontal background velocity). The major features of this flow are clearly reproduced by ray calculations. Ray trajectories have been superimposed on the figure and have been obtained using the methods described in Broutman and Young (1986), except that the ray calculations give no indication of the phase. No attempt has been made in these ray traces to model the initial envelope of the internal wave packet, other than to launch rays over the region where this wave packet has significant amplitude. The location of the major refraction, where the ray path bends sharply, corresponds to the depth where the phase velocity of the inertial wave equals the group velocity of the short wave packet.

Figure 2 shows the time evolution of the vertical wavenumber energy spectra. Each of these spectra is the average over the previous six hours. In all cases, the energy associated with the original background inertial wave is subtracted out. The spectra are then normalized so that the integral with respect to mode number at time zero is unity, integrating only over positive wavenumbers. After a day or so the spectral form is fairly well established and the potential and kinetic energy associated with small-scale waves is approximately equi-distributed.

In Figure 3, the vertical wavenumber energy spectra averaged over the whole time period of the calculation are displayed. It is apparent that there is a well-defined m^{-2} region of the spectrum from a scale of about 15m down to about .3m, after which there is an exponential decay of energy. Also shown in the figure are the spectra for a run where the initial vertical wavenumber of the short internal wave packet was given by $m/k = -1$, and one can see that the same general behaviour, although for scales larger than 15m the m^{-2} slope is less clear.

4. CONCLUSIONS

Numerical simulations of the interactions of small scale waves with large scale inertial waves have been performed. These simulations have confirmed the earlier ray-theoretic work of Broutman and Young (1986) and have shown how the critical layer absorption predicted in earlier work with time-invariant shear is modified by the presence of rotation. This has particular relevance to the mechanisms of breaking and hence dissipation of internal waves. Future work is required to determine how, and with what frequency, breaking takes place in the presence of rotation when the internal wave amplitudes are larger.

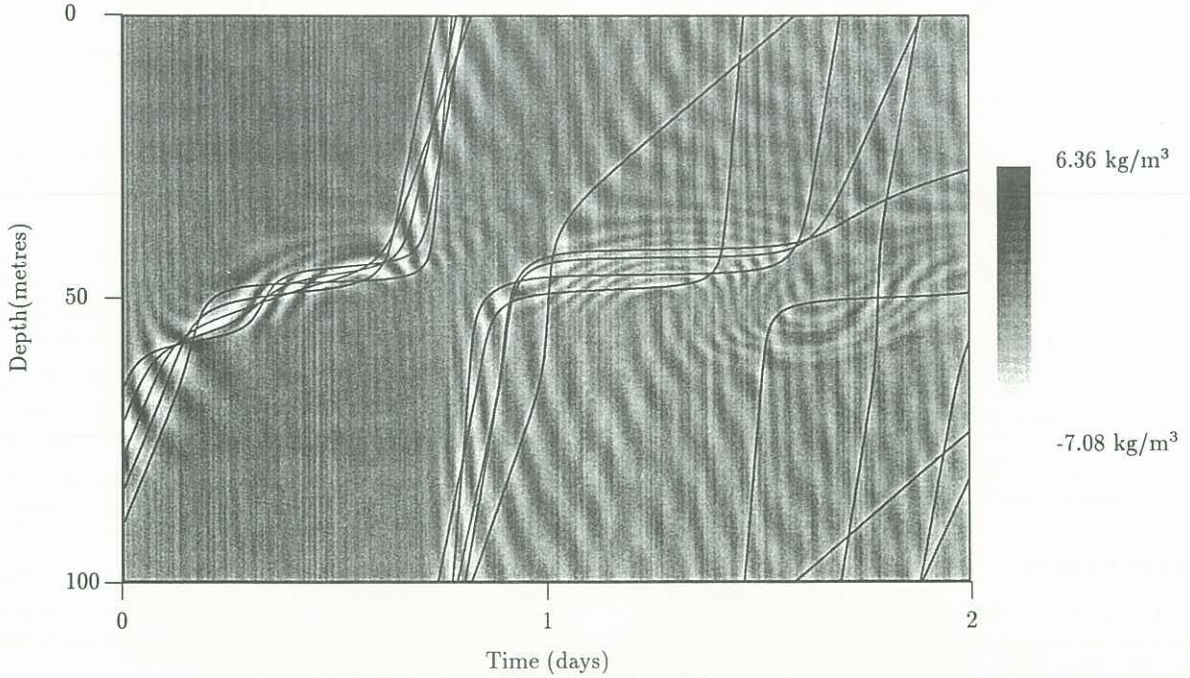

Figure 1. Perturbation density as a function of depth and time, showing an internal wave propagating upward and interacting with the time varying shear due to the presence of an inertial wave centred at a depth of 50m. The ray paths overlaid have been calculated using the methods described in Broutman and Young (1986).

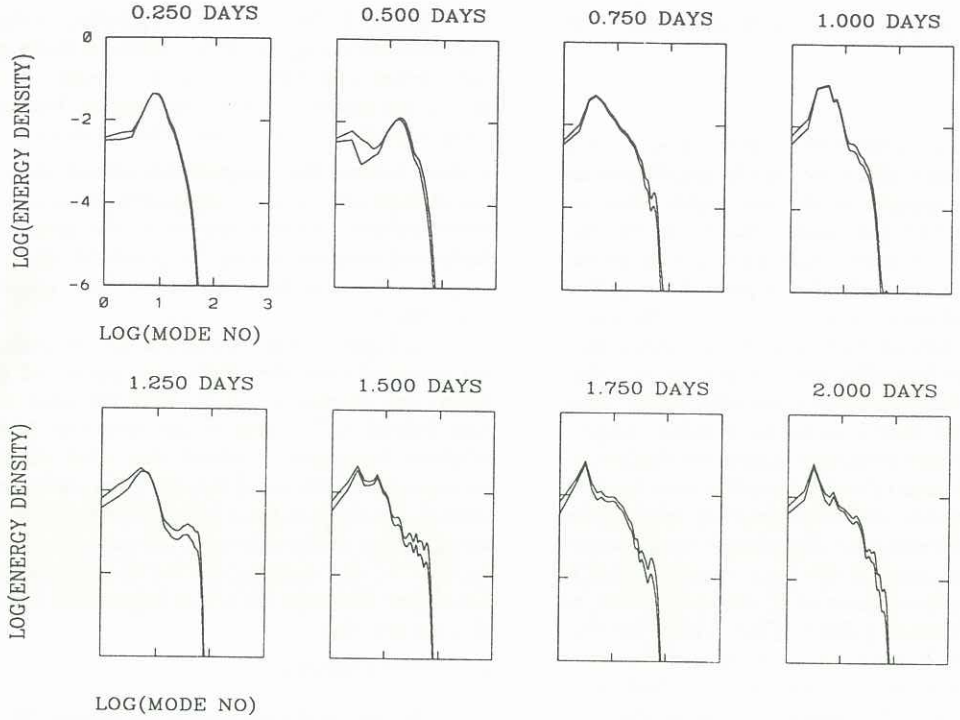

Figure 2. A sequence of vertical wavenumber energy spectra showing the evolution of a power law spectrum from an initial narrow-band wave packet. Both potential and kinetic energy and shown; in each case the kinetic energy level is slightly greater. (The logarithms are base 10).

It has also been demonstrated that refraction is a robust mechanism for generating power law energy spectra in relatively short periods of time.

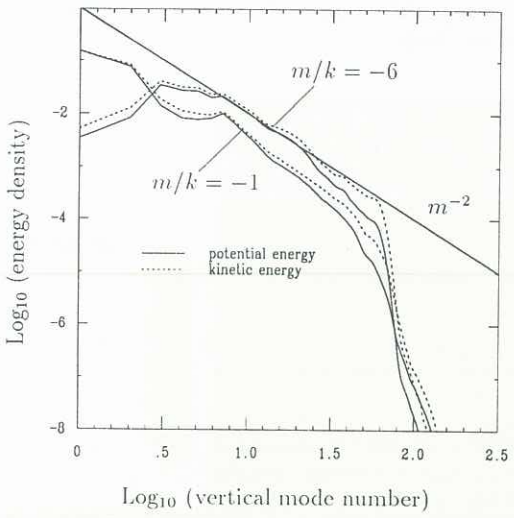

Figure 3. The time averaged vertical wavenumber energy spectra.

5. REFERENCES

BROUTMAN, D. (1984) The focusing of short internal waves by an inertial wave, Geophys. Astrophys. Fluid Dyn., 30, 199 – 225.

BROUTMAN, D. (1986) On internal wave caustics, J. Phys. Oceanogr., 16, 1625 – 1635.

BROUTMAN, D. and YOUNG, W.R. (1986) On the interaction of small-scale oceanic internal waves with near-inertial waves, J. Fluid Mech., 166, 341 – 358.

BROUTMAN, D. and GRIMSHAW, R. (1988) The energetics of the interaction of short small-amplitude internal waves and inertial waves, J. Fluid Mech., 196, 93 – 106.

GARRETT, C. and MUNK, W. (1979) Internal waves in the ocean, Ann. Rev. Fluid Mech., 11, 339 – 369.

HENYEY, F.S., WRIGHT, J. and FLATTÉ, S.M. (1986) Energy and action flow through the internal wave field: an eikonal approach, J. Geophys. Res., 91 (C7) , 8487 – 8495.

HOLLOWAY, G. (1984) Probing the internal wave strong interaction regime by numerical experimentation, in J. Internal Gravity Waves and Small-Scale Turbulence, 221 –248, Eds. P. Müller and R. Pujalet.

MÜLLER, P., HOLLOWAY, G., HENYEY, F. and POMPHREY, N. (1986) Nonlinear interactions among internal gravity waves, Rev. Geophys., 24, 3, 493 – 536.

SHEN, C. and HOLLOWAY, G. (1986) A numerical study of the frequency and energetics of nonlinear internal gravity waves, J. Geophys. Res., 1, 953 – 973.

WINTERS, K.B. and D'ASARO, E.A. (1989) Two-dimensional instability of finite amplitude internal gravity wave packets near a critical layer, J. Geophys. Res., 94, C9, 12709 – 12719.